Continuously Variable Orifice Extrusion for Build Time Reduction in Fused Filament Fabrication Additive Manufacturing

by

Osama Habbal

A thesis submitted in partial fulfillment
of the requirements for the degree of
Master of Science in Engineering
(Mechanical Engineering)
in the University of Michigan-Dearborn
2021

Committee Members:

Assistant Professor Christopher Pannier, Chair
Associate Professor German Reyes-Villanueva
Associate Professor Chinedum Okwudire, University of Michigan

Osama M. Habbal

ohabbal@umich.edu

ORCID iD: 0000-0003-1224-2464

Dedication

I dedicate this thesis:

To my dear family who passionately supported me throughout my educational journey and believed in me even when I did not.

To Dr. Reem Khalil, Ahmad Farhat and Dr. Christopher Pannier for their continued support and unwavering belief in my work.

Acknowledgements

I would like to give acknowledgement to all the instructors and teachers who helped me arrive to this level in my educational journey. Special thanks to my advisor, Dr. Christopher Pannier, for his patience with my crazy and random ideas. Special thanks to Dr. Reem Khalil and Ahmad Farhat for their continued encouragement that kept me going through the toughest of times.

Finally, my highest gratitude goes to my loving siblings, to my dear mother and my late father.

Table of Contents

List of Tables

List of Figures

Abstract

Fused filament fabrication (FFF) is an additive manufacturing technique that extrudes string-like polymeric material through a fixed orifice diameter to build an object layer by layer. This process can last from minutes to hours depending on the size and complexity of the geometry. The selected orifice diameter balances between the possible extrusion widths, extrusion height, and material flow rate. Typically, the selected orifice extrusion width is limited to 130% of its diameter while the extrusion height is limited to 70% of the selected orifice diameter. These limits cause a toolpath design tradeoff between high print speed and fine print resolution. This work presents the design of a mechanism that can vary its orifice diameter to provide continuously variable orifice extrusion (CVOE). The mechanism uses a moving shutter to vary the cross-section area that the material can flow through. Additionally, we demonstrate a novel concept that provides CVOE benefits using a nozzle of a fixed size. The "virtual nozzle" system overextrudes lines that are wider and thicker than what the nozzle is than typical bead widths produced at the given nozzle size. In some cases, test prints completed using the virtual nozzle system can provide up to 40% reduction in print time while maintaining good surface resolution. Overall, this work breaks the tradeoff between speed and resolution, giving faster prints while maintaining or increasing the surface resolution.

Chapter 1 Introduction

Additive manufacturing (AM) encompasses a diverse set of techniques to produce 3D structure in a deposition-by-deposition manner starting from a feedstock (often in filament, granule, powder, rod, or strip form), and is commonly called 3D printing. Due to its simplistic mechanical design and operating concept, FFF 3D printing has become the de facto choice of many hobbyists and companies small and large. In some cases, fused filament fabrication (FFF) AM has been used to produce tooling. However, for the most part, FFF has been limited to small scale production or prototyping purposes. For FFF to become viable for medium sized production runs, two issues need to be solved: anisotropy and speed. The first issue, the anisotropy of mechanical properties of the 3D printed parts, results from the inter-layer bonding strength between layers being roughly 50% of the strength of the part in the perpendicular direction to the Z axis (Fayazbakhsh et al., 2019). The second issue, the relatively slow speed of producing a 3D part through a lengthy sequence of numerically controlled depositions of 2D beads of material, adds cost in the form of a longer cycle time for each part than if the part was produced by a conventional manufacturing technique such as injection molding. The cycle time for each FFF AM part is conveniently broken up into times spend to deposit different types of print features. The major print features for most parts are:

1) outer perimeter: the outside “wall” or “shell” of the print not including top or bottom layers;
2) inner perimeter: the inner shell that is directly to the inside of the outer perimeter;

3) infill: the structure that sparsely fills the inside of the part;

4) top layers: the top solid layers of the part; and

5) bottom layers: the bottom solid layers of the part.

For example, the cube shown in Figure 1, breaks down the required print time for each print feature. Subfigure A shows the print time distribution with rectilinear infill, while subfigure B shows the print time distribution with gyroid infill. The figure attempts to shows that the major contributors to the required print time (in order) are infill (labeled “internal infill”), outer perimeter (labeled “external perimeter”), and inner perimeter (labeled “perimeter”).

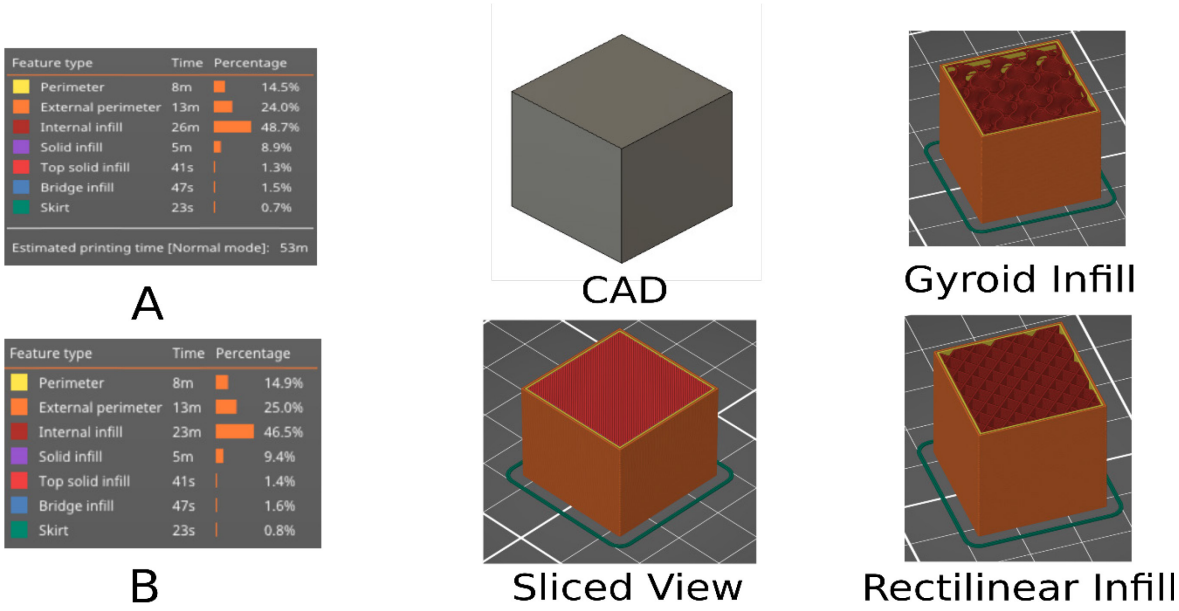

Figure 1 Breakdown of the time required for FFF print features.

This breakdown inspires us to reduce the amount of time that is required by infill and perimeters. This can be done using a large nozzle that can extrude thick and wide beads of material. This however introduces its own set of challenges. As the extruder nozzle cross section is circular, the sharpest corner radius is limited by the radius of the installed nozzle itself. This

effectively limits the size of the object's features to those with a minimum size that are larger than the radius of the nozzle diameter. In Figure 2 this limitation is demonstrated.

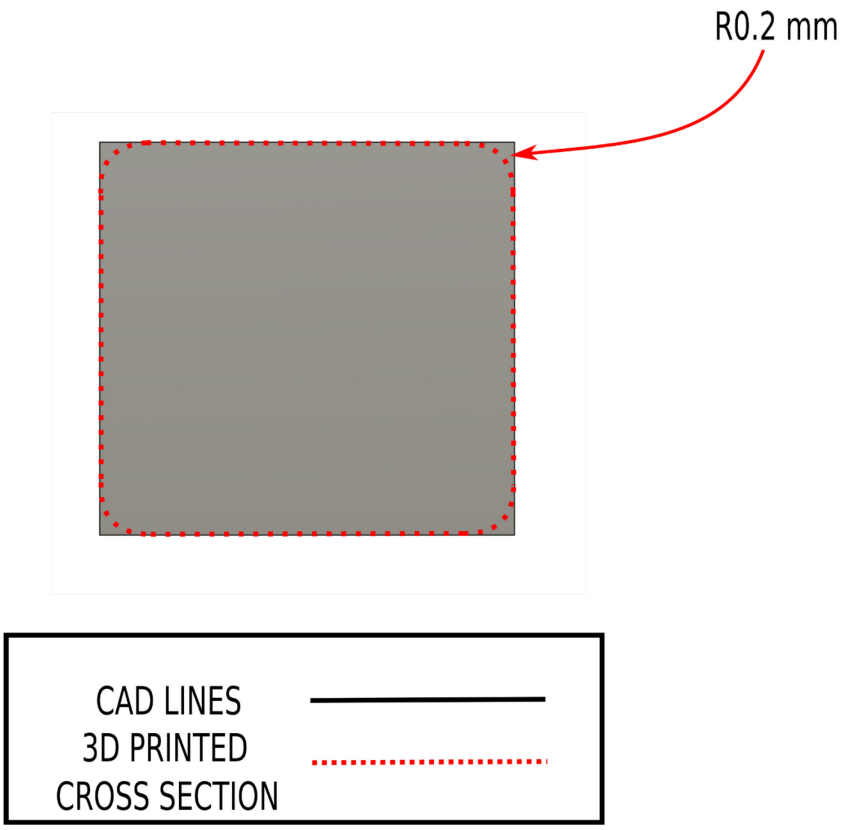

Figure 2 Resolution limits using a fixed nozzle diameter.

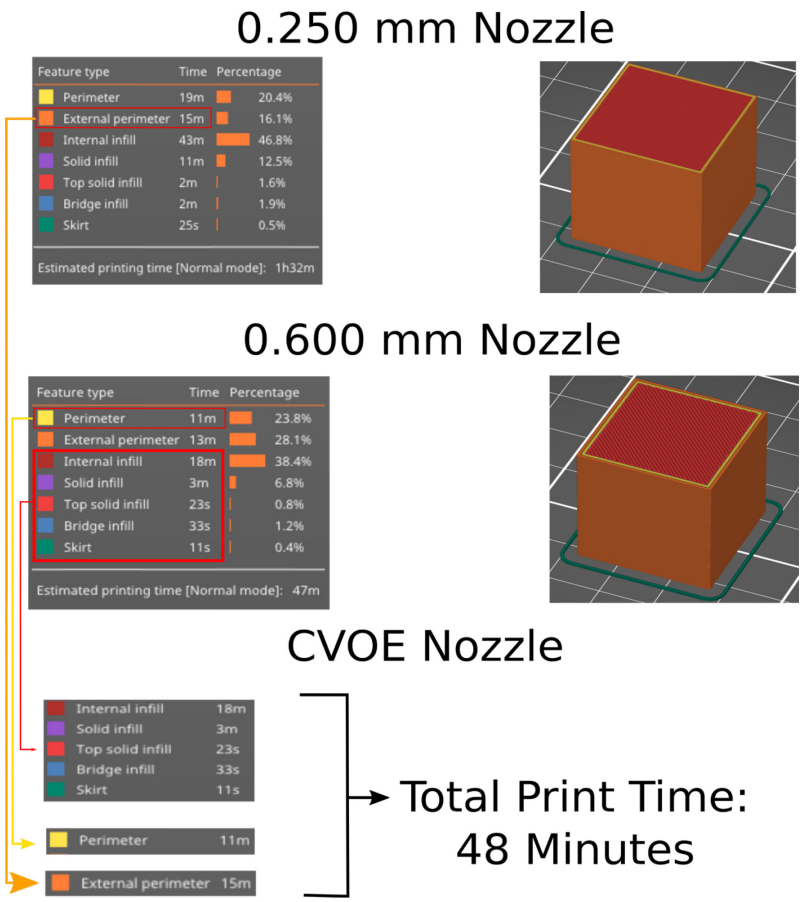

Figure 3 Print time comparison for a 25 mm^3 cube using two nozzle diameters.

The first two subfigures of Figure 3 demonstrate the advantage in time savings when using a large nozzle, however, as mentioned before, this advantage comes at the cost of resolution. This dichotomy can be rectified by using a new nozzle that has the ability of continuously changing its orifice cross-sectional area. In this case, the object is divided into different sections depending on their minimum feature size. For sections requiring high resolution (including small features), a small orifice is used, while large structures and primitive sections are printed using a large orifice (often including internal features). Using this method, the printing time is reduced while maintaining the required resolution.

As a system, a FFF printer is a polymer extrusion system coupled to a motion stage. This means that it suffers from the same issues that exist in other extrusion systems, including die

swelling and flow instabilities. Die swelling involves an extrudate output that is of a larger dimension than the die. Additionally, at high flow rates, the flow can experience some flow instabilities due to turbulent flow formation, the resulting flow structures show features like shark skin or melt fracture. Yet, between the regions of stable and unstable flow, there is a range of flow rates that can be used to provide bead widths and heights that are beyond the industry standard 100%~130% of the nozzle diameter for the width and 30%~70% of the nozzle diameter for the height with minimal deleterious effect from die swelling or flow instability. In this novel concept for continuously variable orifice extrusion (CVOE), the velocity of the extruder can be varied relative to that of the X-Y stage to obtain the benefits of a larger nozzle diameter while using a smaller diameter nozzle.

This work presents the theory of operation, mechanical design, and testing results of our VOE and CVOE system and the novel CVOE system.

Chapter 2 Literature Review

Current FFF AM machines suffer from slow build times when compared to injection molding. FFF AM is usually compared to injection molding as both are primarily used for polymers. Additive manufacturing in mass production affords the factory a great flexibility and a low production line setup cost. This is in part due to the lack of the need to produce customized molds and tooling for the specific production application. The maximum flow rate afforded by FFF printers is three to four orders of magnitude smaller than injection molding machines (Rajamani et al., 2021). This limits the production rates, which is one of the main contributors to part cost in manufacturing. Other cost contributors include raw material cost, setup cost, and machine capital cost (Thomas & Gilbert, 2015). The setup cost for additive manufacturing is comprised of the cost of creating toolpaths for the part and setting up of the build plate and the correct material for the part. This cost is significantly lower than the equivalent injection molding process, for which molds need to be designed and produced, and a lengthy optimization process of the injection shots must be conducted (Rajamani et al., 2021). On the other hand, injection molding of the cubic piece previously shown in Figure 1 requires a cycle time in the seconds range while an FFF printer will require a build time in the minutes range. The resulting parts may look similar overall, however, the 3d printed part will possess some visible layer lines and looser tolerances when compared to the injection molded part. Solving this problem requires a new tool that can provide both a high extrusion rates and high resolution. A CVOE printhead

will provide customizable output cross-sectional area to suit the resolution requirement for the section being printed.

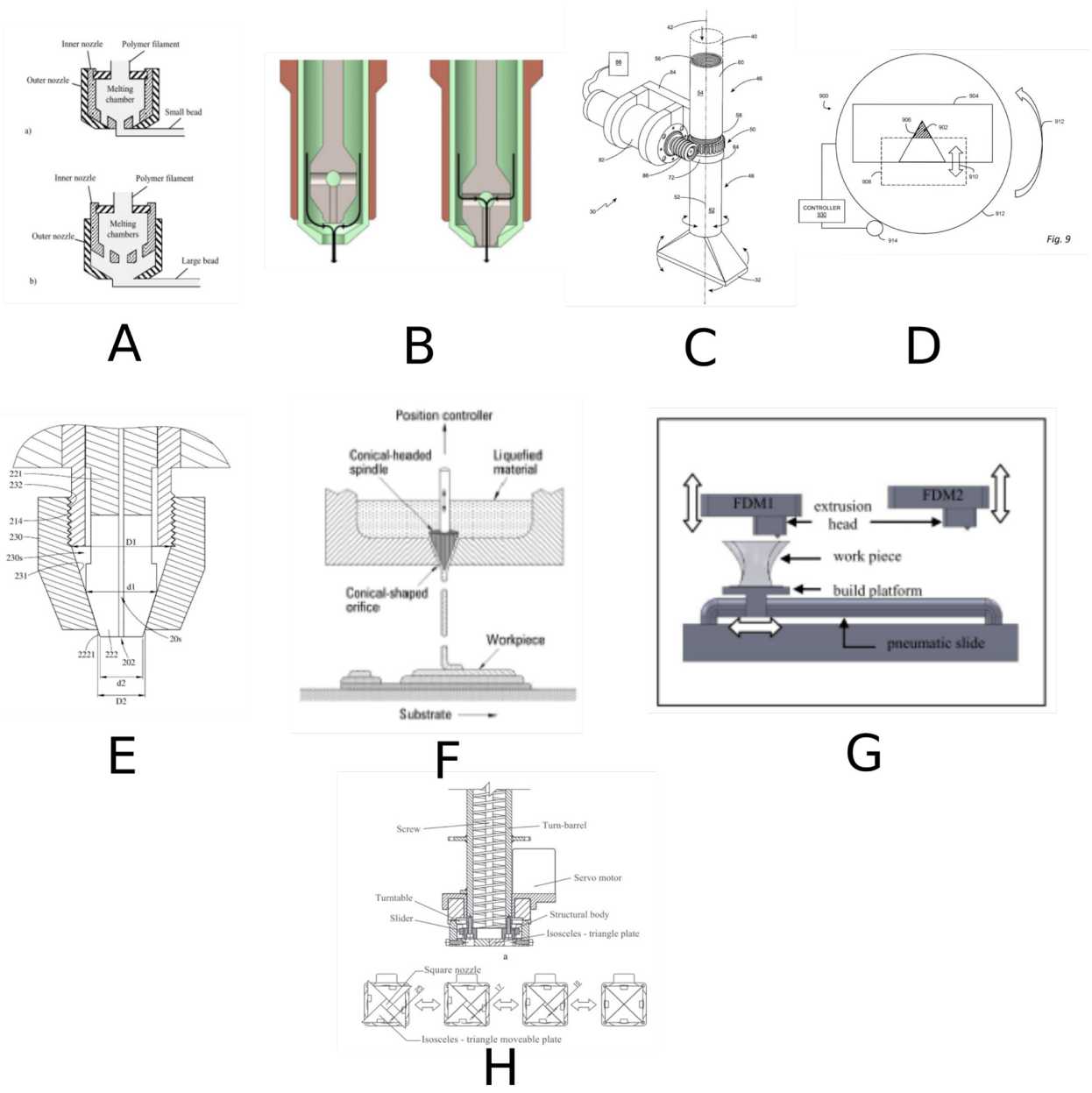

Figure 4 Prior work on VOE and CVOE systems.

The concept of a multi output resolution print head was first introduced by Brooks et al. in 2011. The paper outlines a print head with multiple coaxial cylinders. When a low resolution is required, the inner cylinder retracts, exposing a larger output cross sectional area (Figure 4A).

This design was later built and tested by Oak Ridge National Laboratory (Figure 4B), and cylinders with diameters of 2.5 mm and 7.6 mm were used (Chesser et al., 2019). Other designs showed the concept of a rectangular nozzle, when high resolution is required, the shorter side of the rectangle is aligned with the direction of travel to print thin lines (Figure 4C). For low resolution, the longer side of the rectangle is aligned with the travel direction to provide wide extrusion width (Lind et al., 2016). This method provides a wide range of extrusion widths; however, the extrusion height is limited. Myerberg et al. investigated a triangular shaped orifice with a shutter, the shutter moves to expose or cover part of the triangle, thereby increasing or reducing the output cross sectional area (Figure 4D). Another design describes a collet and nut mechanism. The collet nut has a tapered inner surface that pushes against an inner collet causing it to contract, thereby reducing the output diameter (Figure 4E). The process can also be reversed to produce large output diameters (Teng - Yen WANG, 2018). A hole and cone insert mechanism was investigated, the cone has the capacity to move in the axial direction and has the material flow around it (Figure 4F). As the cone is inserted into the orifice, the flow diameter widens. This mechanism allows for the variation of extrusion widths from 12 mm to 2 mm (Tseng & Tanaka, 2001). A multi print-head mechanism was designed and tested (Figure 4G). The resulting mechanism contained four independent print heads with a moving platform that can move between two pairs of print heads. Each print head contained a separate orifice size that provided a specific extrusion width (Espalin et al., 2012). Xu et al. details the design of a nozzle with four isosceles plates that slide against each other to vary the output cross section. The extruder was used to print structures made with concrete (Figure 4H).

The literature provides an ample number of concepts and theoretical models of various VOE mechanisms. However, most of the previously mentioned concepts do not present

experimental data and real-world testing. Moreover, concepts that vary the feed rate of the extruder relative to the X-Y-Z stage feed rate allow for a some of the benefits of VOE and CVOE systems with very minimal or no hardware modifications.

Chapter 3 System Design for Variable Orifice Extrusion

In this chapter, we discuss the design and build of our variable orifice extrusion system. Varying the physical orifice cross-sectional area can be achieved by two methods: 1) discrete variation of the output cross-sectional area, and 2) continuous variation of the output cross-sectional area. Examples of the first type can be found in the works of Brooks et al., Espalin et al., and Chesser et al. In discrete variation of the output cross section, the output diameter is varied in fixed steps. This process is demonstrated in Figure 5 in which the multiple orifice diameters correspond to different extrusion widths and heights. Extrusion width is the width of the bead deposited by the extruder. For a given orifice diameter, the value of extrusion width is limited to within a finite range of values for each orifice diameter.

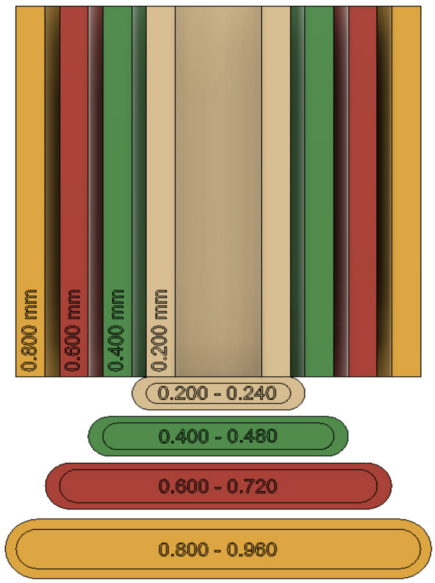

Figure 5 Extrusion width of various nozzle diameters.

Discrete VOE systems can take multiple forms, Chesser et al. demonstrated a design that is based on concentric cylinders. This design can switch between two discrete nozzle sizes. Figure 6 shows the design operational concept.

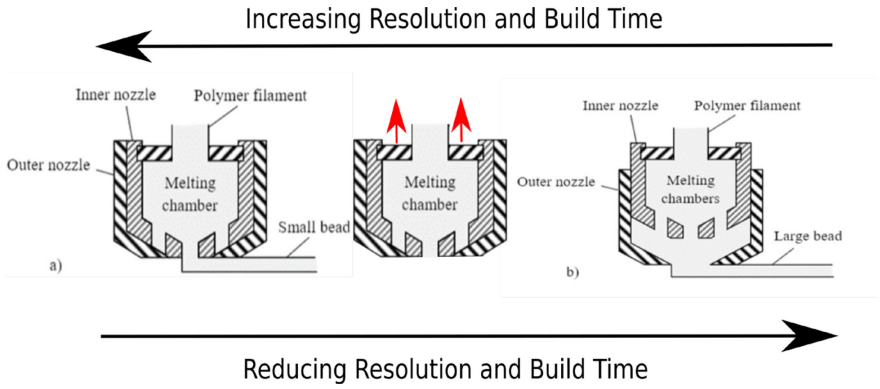

Figure 6 Chesser et al. discrete VOE system.

3.1 Turret Based VOE System Design

To achieve variable orifice extrusion, we designed and built a turret-based VOE system. The system was built by repurposing a desktop FFF 3D printer and installing our customized print head on the X-axis. The print head combined four features: 1) a rotating turret containing multiple secondary nozzles with different orifice diameters, 2) a solenoid mechanism to raise and lower the turret, and 3) a nozzle selection mechanism containing a stepper motor and a gear train, 4) a cam and a snap action limit switch indicate the home position of the turret, which corresponds to the smallest secondary nozzle. The VOE printhead is mounted on the X-axis gantry of a modified desktop FFF printer (Creality Ender-3 Pro, Shenzhen, China).

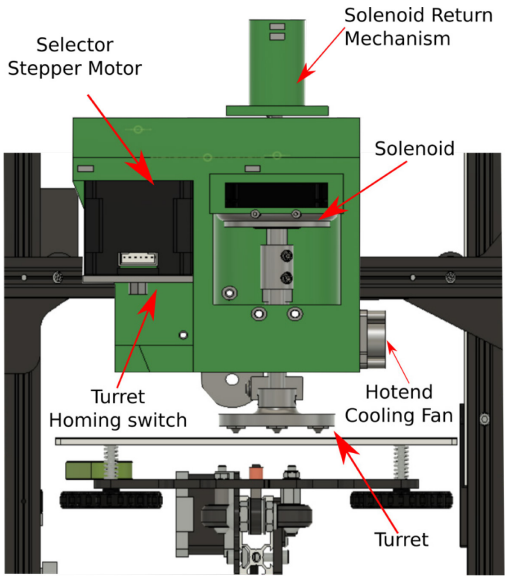

Figure 7 VOE print head mounted on a Creality Ender 3 desktop FFF 3D printer.

The seal for the molten polymer as it flows from the primary to secondary nozzle is achieved via a cup and cone geometry of the metal nozzles as shown in Figure 8. The turret is comprised of the turret disk and four secondary nozzles.

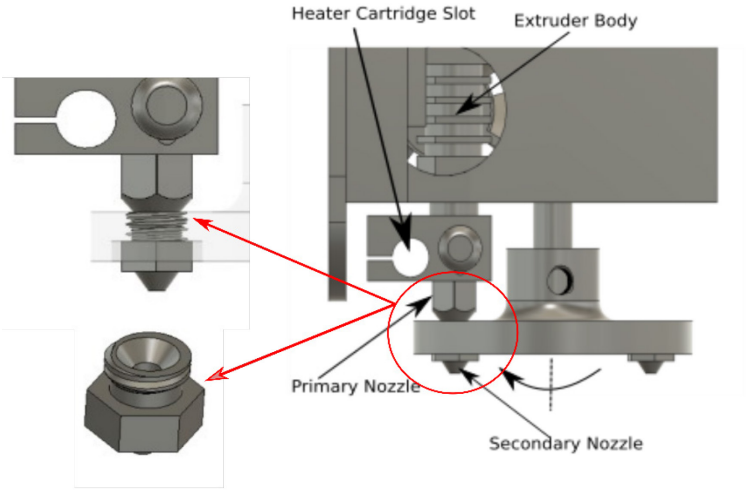

Figure 8 Cup and cone seal between the primary and secondary nozzles.

The nozzles were made by shortening standard E3D V6 nozzles (E3D Ltd., Oxfordshire, UK), milling approximately 4 mm off from the inlet of the secondary nozzles and machining a cup geometry to seal against the conical frustum of the primary nozzle. The turret material is titanium, a metal with relatively low thermal conductivity, to reduce heat loss from the primary nozzle and reduce the effects of thermal expansion. Figure 9 shows the primary parts of the print head.

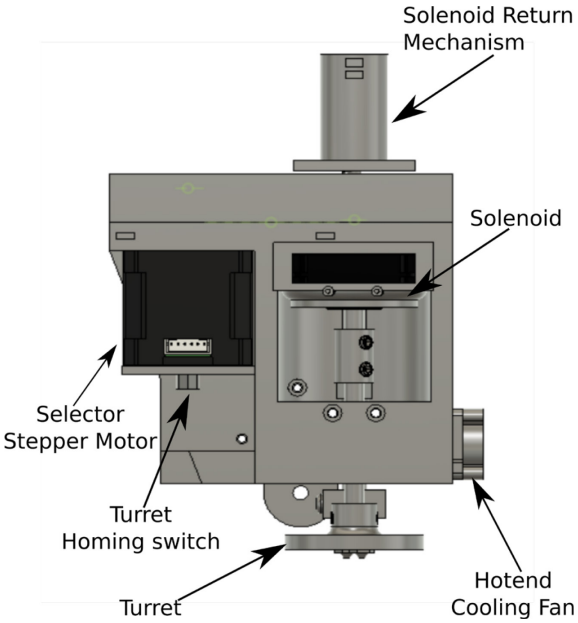

Figure 9 Isolated view of the extruder assembly.

The system is controlled by a Duet3D Duet 3 Main Board 6HC (Duet3D Ltd., Peterborough, UK) through the Duet3d web interface. The solenoid is controlled through an auxiliary H-bridge motor driver integrated circuit. The print head has two cooling fans: the first to cool the extruder heat sink and the second to cool the solenoid and prevent it from overheating. Rotation from the stepper motor is linked to the turret shaft via a geartrain with an effective gear ratio of 1:1. The turret is lifted by the solenoid which causes the secondary nozzle

to seat into the primary nozzle. To unseat the two nozzles, a turret return spring provides force to push the turret down. Details of the geartrain and the return spring are shown in Figure 10.

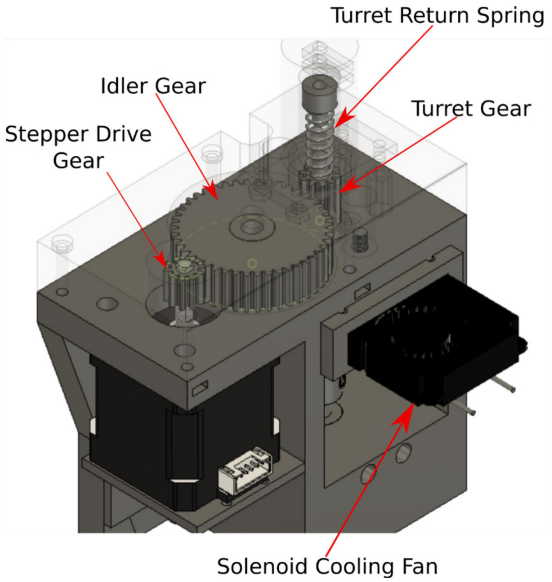

Figure 10 Top view of the VOE system showing geartrain, turret return mechanism, and cooling fan.

The standard firmware of the Creality Ender 3 was modified to include the G-code for tool switching. The "Tool Change" G-code starts by 1) raising the Z-axis by 10 mm, 2) de-energizing the solenoid, thereby dropping the turret approximately 6 mm, 3) activating the selector stepper motor and rotating by a set number of angular steps to select the desired nozzle, 4) energizing the solenoid, and finally 4) lowering the Z-axis by 10 mm to resume printing. A video showing a tool change operation is available at the following URL: https://youtu.be/zvoY7zORnzQ.

Preparing objects for use with the VOE system was done in the following steps. In the CAD software, the object is first divided into different sections depending on their detail level. These objects are then saved and exported as STL files. The files are then imported into the slicing software simplify3D. In simplify3D, different "processes" are created for each secondary

nozzle size. As the model is imported and arranged in simplify3D, its different sections are assigned to different processes depending on their individual resolution needs. Figure 11 details the workflow required used with the VOE system.

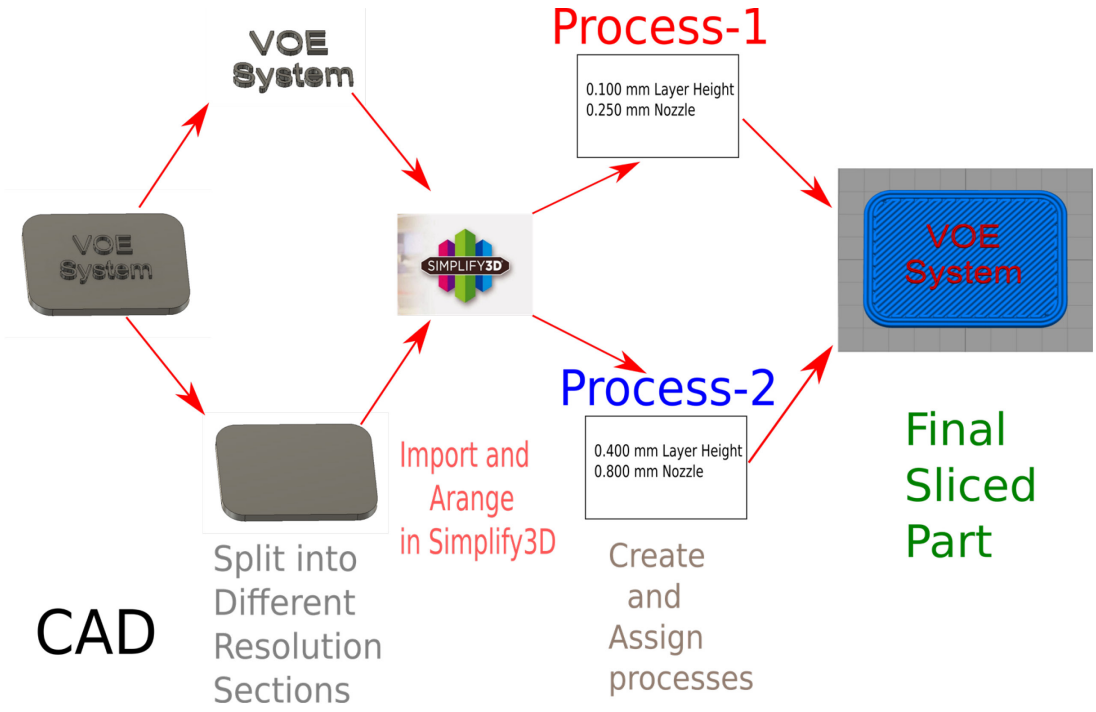

Figure 11 Object preparation for VOE system.

3.2 An Improved Turret-Based VOE System Design

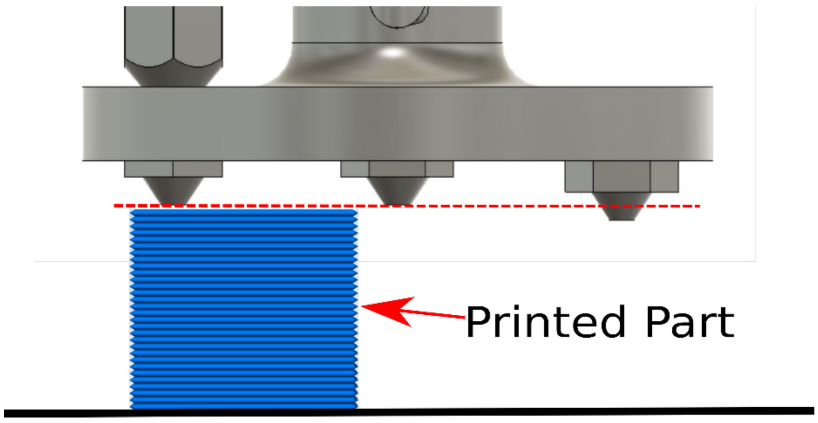

Figure 12 Unlevel secondary nozzle that could conflict with the printed part.

Testing of the turret-based VOE system revealed limitations of the secondary nozzle-switching mechanism. The first issue related to the positioning of the secondary nozzles, where collisions due to unlevel secondary nozzles as shown in Figure 12 . While the nozzles are initially at the same height, once a nozzle is used, it expands due to heat. This expansion can lead to collisions once the nozzle is switched. The second issue manifested itself as print artifacts, these artifacts can be traced back to the large mass of the print head. To remedy these issues, multiple changes were made: 1) removal of the stepper motor and solenoid, 2) addition of a selective nozzle-lowering mechanism. Design improvements were incorporated into an improved VOE system to ensure that the active secondary nozzle was always the lowest point on the turret and to reduce mass of the print head. In place of the motor and the solenoid, a novel belt driven mechanism was designed. The basic functions of this mechanism depend on two pulleys, one pulley-drive is responsible for raising and lowering the turret, while the other drive-pulley is responsible for rotating the turret. The various parts of the pulley drive system are shown in Figure 13.

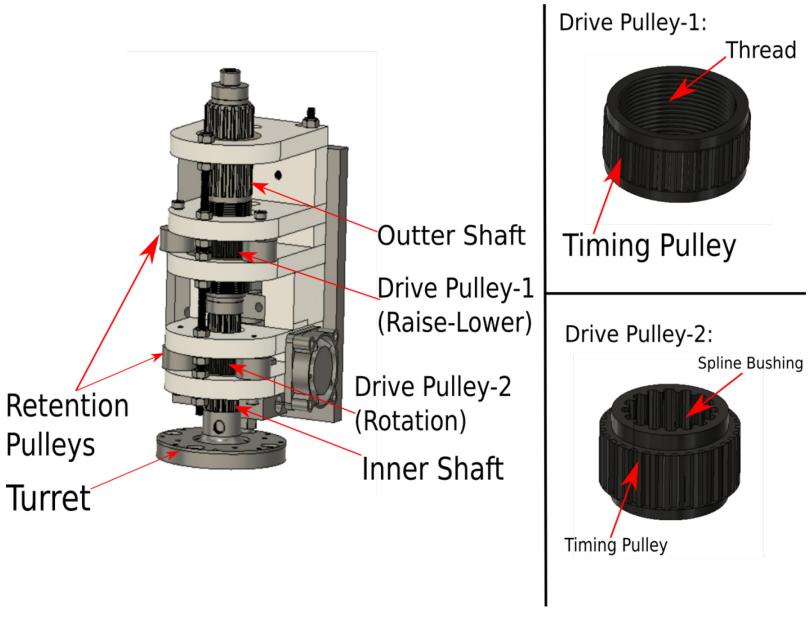

Figure 13 VOE V2.0 belt driven raise-lower-rotate mechanism.

Drive pulley-1 has a low-pitch thread on the inside surface and miniature extra light (MXL) timing teeth on the outside, the inner threads ride along the threaded section of the outer shaft; this facilitates the raising and lowering motion of the turret. To ensure that the outer shaft does not rotate while drive pulley is rotated, the outer shaft has a splined upper section which rides along a splined bushing at the top of the mechanism. Drive pulley-2 facilitates rotation of the turret, as the pulley is rotated via a belt, the splined inner section of the pulley rotates the inner shaft and thus, the turret. To rotate the drive pulleys, timing belts and two stepper motors are used. By mounting the stepper motor on the X-axis and driving the nozzle-switching motions via belts, the overall weight of the printhead is reduced compared to the previous design using a solenoid. However, this novel drive mechanism requires three specific drive modes for the three carriage motors. Table 1 outlines the running behavior during the three operations: rotation, raising/lowering, and printing.

	X-Carriage Motor	**Drive Pulley-1 Motor**	**Drive Pulley-2 Motor**
Printing	Active (initiator)	Active (follower)	Active (follower)
Lowering/ Raising Turret	Inactive (Brake on)	Active	Inactive
Turret Rotation	Inactive (Brake on)	Inactive	Active

Table 1 Stepper motor operational modes under the different functions of raising-lowering-rotating.

The active lowering mechanism works by suspending the nozzle insert upon a spring washer inside a counterbored hole in the turret body. When the turret is raised, the primary nozzle pushes against the secondary nozzle. This action deforms the spring to lower the selected secondary nozzle. This mechanism ensures that inactive secondary nozzles do not collide with the printed object. To reduce the switching time, the time to reheat the selected nozzle will be reduced by using a smaller and lighter secondary nozzle assembly. This reduces the thermal

mass of the secondary nozzle and thus the heating time. Figure 14 shows the redesigned nozzle as well as its operating mechanism.

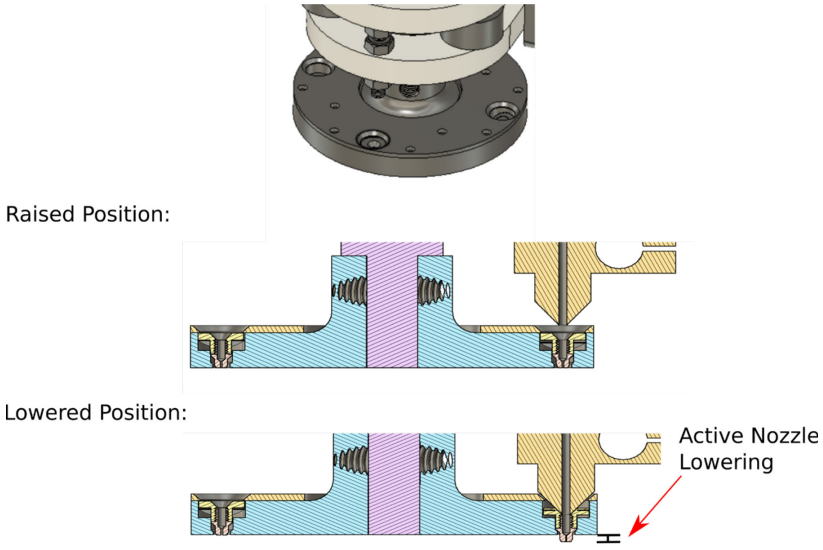

Figure 14 Sectional view of the lowering mechanism for only the active nozzle of the improved turret-based VOE system.

3.3 A Continuously Variable Orifice Extrusion System Using a Sliding Shutter

The two preceding system are systems that are only capable of discreet cross-sectional changes. This upcoming system can provide a continuous change in the output cross section. This continuous variation increases the effectiveness of the standard VOE system. A CVOE system eliminates the nozzle change time and has the potential for new actuation to reduce dynamic errors in the extrusion. In discrete VOE, the point along the extruded bead at which the print head changes nozzles is subject to an extrusion discontinuity that reduces the overall quality of the print. Examples of CVOE from literature include the work done by Lind, Meyrberg, Wang, Tseng, and Xu. This design uses a square nozzle orifice and a square shutter that exposes or covers part of the square orifice, giving a square area that is actuated by changing the diagonal length of the square. The shutter is mounted on two compact dovetail linear stages (Newport,

Irvine, CA). A standard E3D V6 nozzle (E3D Ltd., Oxfordshire, UK) was modified to open the 1.0 mm diameter circular orifice to a 1.3 mm side-length square using a 1.3 mm square micro rotary broach (Polygon solutions, Florida, USA), operated through linear broaching. Variation of the position of the shutter is done by moving the two dovetail stages using the MXL pulley mounted on the drive screw for each stage. Power is transmitted to the pulleys via a belt driven by a stepper motor. The home position of the shutter is the position at which the shutter uncovers the square nozzle output completely, as shown in Figure 15. The home position of the shutter is probed using a snap switch mounted to the dovetail stage end. Z-axis homing is completed using a hall effect limit switch (AntClabs BLtouch, Seoul, South Korea). Control of the CVOE and the X-Y-Z axis is computed using a Duet3D Duet 3 Main Board 6HC (Peterborough, UK). The shutter actuating motor is setup in the RepRap firmware as the A-axis. Figure 16 highlights the main components of the CVOE system.

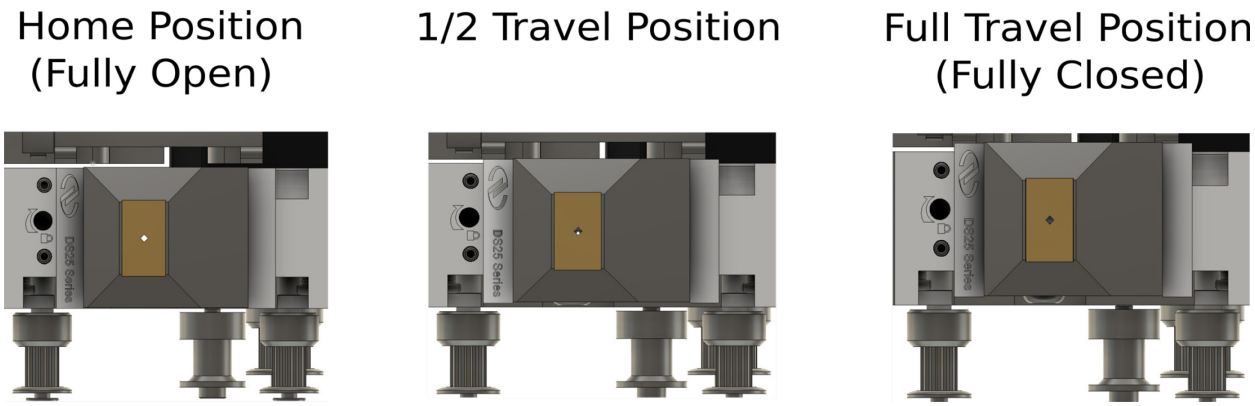

Figure 15 Output cross sectional area relative to the position of the dovetail stages.

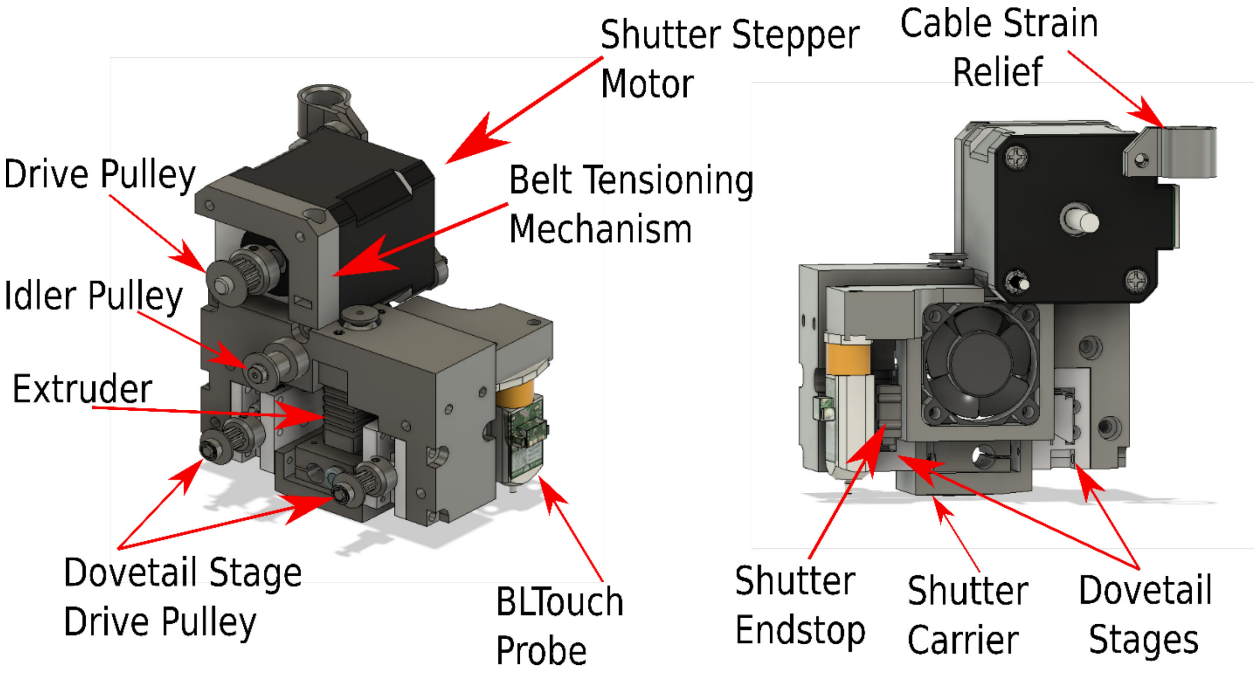

Figure 16 Breakdown of the major components of the CVOE system.

The shutter is comprised of a holder, called the “shutter carrier”, to which a thin piece of shim stock is attached. The shutter contains a rectangular hole of the same size as the nozzle. The shutter shim is mounted to the shutter carrier via a soldering process. Both the shutter and the shutter carrier are made of low carbon steel. The shim shutter assembly is shown in Figure 17.

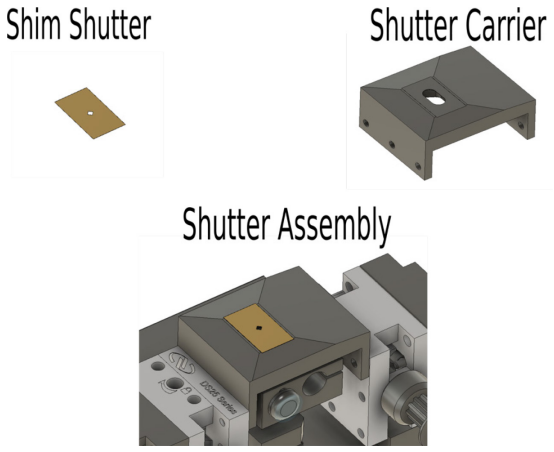

Figure 17 Shutter components and assembly.

During operation, as the stepper motor is rotated, and, in turn, rotates the dovetail stage pulleys, the dovetail stages move forward closing off the square nozzle. Figure 15 visualizes this process. The change of cross-sectional area in this system consumes less time when compared to the VOE system and unlike the VOE system, no artifacts are left on the print where the nozzle switch operations are conducted.

Chapter 4 Testing and Validation of Turret-Type VOE System

This chapter presents testing and validation of the initial turret-type VOE system, which is performed by printing a test object. The test object is comprised of two opposing frustums and a cylindrical section. Slopes on FFF 3D prints are traditionally of a higher roughness due to the stair stepping effect as shown in Figure 18. The figure demonstrates the larger area underneath the theoretical CAD cross section for slopped walls (shown in yellow) when compared to a wall with the slop of zero (shown in cyan). This effect can be reduced by reducing the layer height or by non-planar printing.

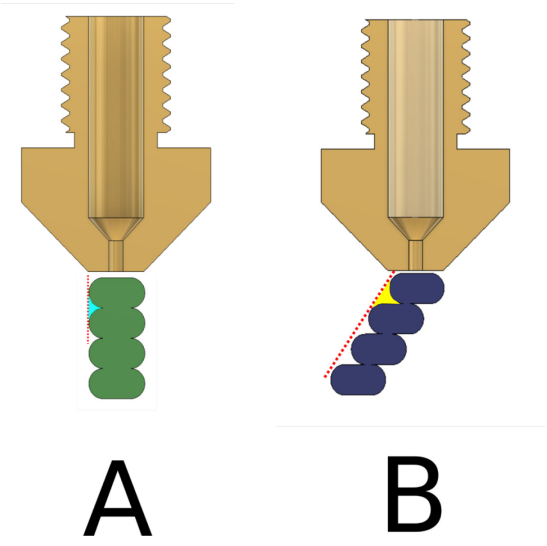

Figure 18 Demonstration of the stair stepping effect in 3D printing.

The slopped sections in the test coupons highlight the resolution difference between using two different secondary nozzle diameters: 0.80 mm and 0.40 mm. The test shape is shown in Figure 19.

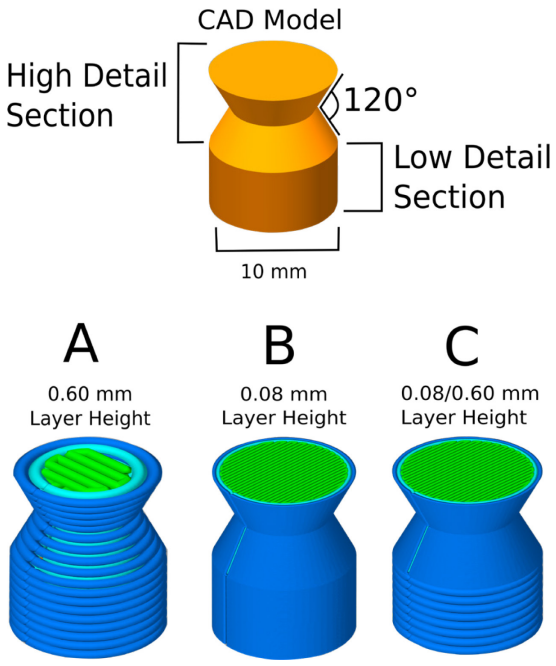

Figure 19 Experimental test setups for the VOE system.

Test coupon A is printed using a 0.80 mm secondary nozzle and a layer height of 0.60 mm. Test coupon B is printed using a 0.40 mm nozzle and 0.08 mm layer height. Test coupon C can only be printed using a VOE system, because the lower cylindrical section is printed using a 0.80 mm secondary nozzle while the upper two “opposing frustums” are printed using a 0.40 mm nozzle. The resulting test coupons were later scanned using a high-resolution laser line profiler with 0.0002 mm Z repeatability (Gocator 2410, LMI3D, Vancouver, BC).

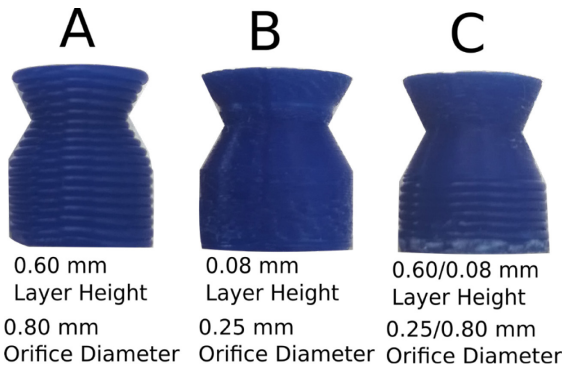

Figure 20 Test coupon results.

The test results, shown in Figure 20, show a predictable result for test coupon A. The resulting print shows low resolution and severe stair-stepping effects on the slopes. Additionally, the transition point from the cylindrical section to the frustums is less pronounced on the printed part compared to the CAD reference geometry. Similarly, the axial position at which the slope is inverted, named the "inflection point", is smoothed-over with a heavy loss in resolution, as shown in Figure 21.

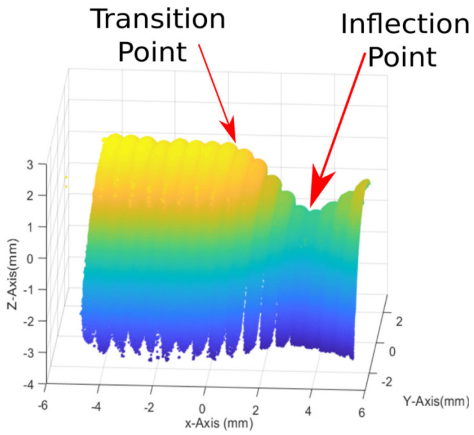

Figure 21 Scan result for test coupon A.

Test coupon B, shown in Figure 22, shows an improvement in quality over test coupon A, stair stepping effects are noticeably less visible than those that are on test coupon A. Additionally, the transition point and inflection are sharper.

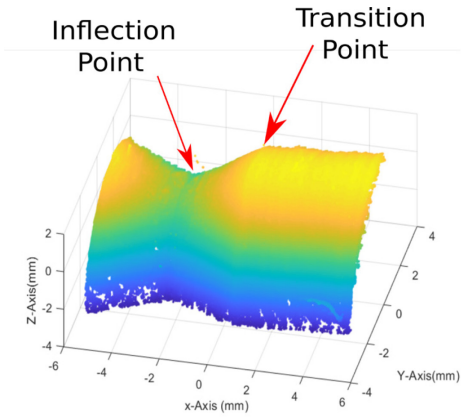

Figure 22 Scan results of test coupon B.

Test coupon C, shown in Figure 23 Scan results of test coupon C, maintains good resolution on the high detail section while reducing the print time by 36%, from 36 minutes for test coupon B down to 23 minutes. The print time values are summarized in Figure 24.

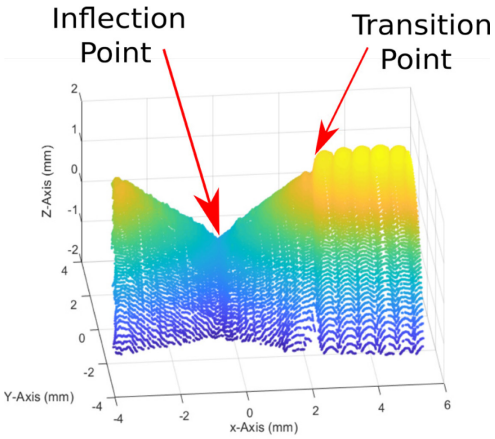

Figure 23 Scan results of test coupon C.

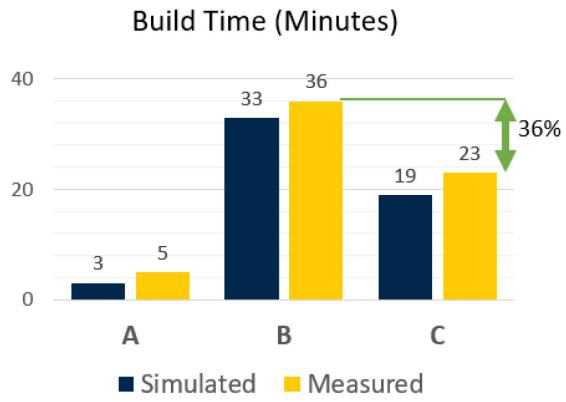

Figure 24 Simulated vs. measured print time for test coupons A, B and C.

Chapter 5 Die Swelling and CVOE Implications

5.1 Introduction to Die Swelling

Die swelling is a rheological phenomenon that is observed in polymers that undergo an extrusion process. Die swelling can be described as the expansion of the polymer flow as it exists the extrusion die. The die swell ratio can be defined as the ratio of the extruded polymer diameter to the diameter of the die. Die swelling is observed in non-Newtonian fluids such as the thermoplastics that are used in FFF additive manufacturing. Figure 25 demonstrates die swelling behavior.

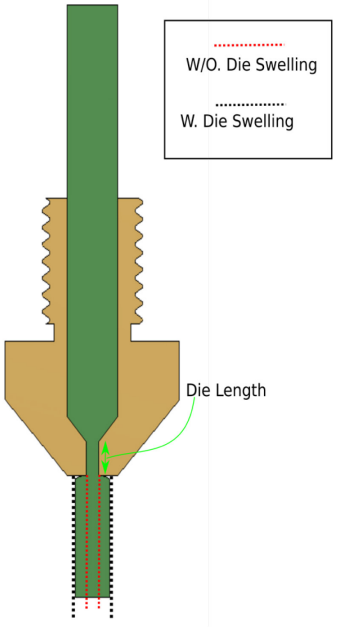

Figure 25 Die swelling behavior.

Die swelling behavior is exacerbated by a high-shear-stress rate, a small die-length-to-die-diameter ratio, a high molecular weight of the extruded polymer, and a high extrusion temperature. In the presented CVOE system design, the die length is the same as the thickness of the shim shutter, making the die length to die diameter ratio equal to 1/40. This small ratio causes a large swell ratio of ~3.25.

Die swelling occurs due to two mechanisms. The first mechanism is related to the molecular dynamics of the flow. The theory assumes the molecules of the polymer melt to act as a spring element. As the flow is forced through a die, the polymer molecules are forced into a dense configuration. The new configuration holds a very high potential energy, which is released the moment the flow exists the nozzle. The act of releasing of the potential energy causes die swelling in the extrudate. The second die swelling mechanism involves the flow velocities of the extrudate. Inside the die, the flow at the walls has a velocity that is zero due to the no-slip boundary condition. This means that the flow has a parabolic velocity profile, yet as the flow exists the nozzle, the flow velocity profile becomes uniform. Regions that had a higher velocity decelerate and regions with a lower velocity accelerate. This has the physical effect of causing the flow to shrink in the Z-direction. Due to the conservation of volume for an incompressible flow, as the flow shrinks in the Z-direction, it must swell in the X-Y direction.

Die swelling causes flow diameter and shape inaccuracies. This can be detrimental in additive manufacturing as slicer programs typically assume the flow width to be that of the physical nozzle diameter. Physically, die swelling can cause extruded lines to be of a width that is thicker than what is set in the slicer software, depending on the input velocity of the filament. In industrial polymer extrusion machines, dies that extrude a square cross section, typically have a non-square cross section; the cross section is designed to account for the swelling that would

otherwise occur at the straight sides of the square. Additionally, circular and annular cross sections are typically extruded using an under sized die such that the output is slightly larger than the die to compensate for the die swelling phenomena and meet the desired tolerance (Kostic & Reifschneider, 2006).

The design of the CVOE system with the movable shutter is highly susceptible to die swelling. The flow coming out of the primary nozzle is subjected to a very sharp constriction. Additionally, this constriction has no appreciable die length where the molecules can be rearranged into a more stable configuration. All factors considered, our first version of the CVOE system suffered from severe die swelling behavior.

5.2 Die Swelling Under a Different Light

So far, we have established that die swelling is a deteriorative side effect for any extrusion-based process. However, the same effect can be used to achieve a continuously variable width and height extrusion. By varying the feed velocity of the filament, the die swelling behavior can be controlled to provide an extrudate diameter that is larger of the physical nozzle diameter. This new diameter is denoted as a “virtual nozzle diameter”. This method can turn any standard FFF 3D printer with a fixed nozzle into a printer with a CVOE system. That said, the maximum possible throughput is limited, as beyond a range of flow velocities, the flow becomes turbulent and experiences instabilities like shark skin. However, for desktop 3D printers, the algorithm to be developed has the potential to provide time savings without requiring extensive hardware modifications. It is important to note that while die swelling behavior can be observed in FFF printers, the method of using a virtual nozzle does not only use die swelling to provide thicker and wider extrusions, but it also depends on the variation the ratio

of extruder velocity to the velocity of the motion axis of the printer. In practice, this provides the condition of "over extrusion". This method is shown in Figure 26.

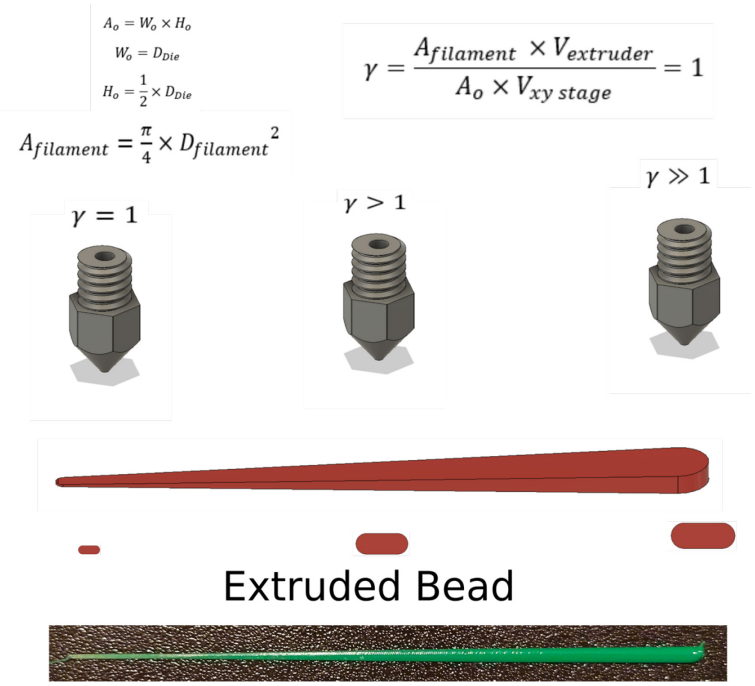

Figure 26 Concept of virtual continuous variable orifice extrusion (VCVOE) system.

The commonly used algorithm in slicing software packages is conservation of volume, where for a given line width, height, and length, the slicer calculates a given volume to extrude. The extruder is treated as a motion axis, however unlike the XYZ axis of the printer, the extruder behaves as a nonlinear second order system. Therefore, the extruder requires a controller to have proper control on its pressure and deposition. This controller is most required for the transient states at the start and end of each extrusion line. Linear Advance is one controller that attempts to ensure extruder pressures and flow rates to be consistent even in regions of acceleration and deceleration (Tronvoll et al., 2019). It assumes a first order system with a K time constant. From our testing, the Linear Advance algorithm functions well within a narrow range of extrusion

widths that are near the installed nozzle diameter. However, the algorithm's performance falls short with extrusion widths that are beyond 130% of the nozzle diameter.

We coin the term "Virtual Nozzle" for extrusions that have a line width that is beyond what the nozzle physically possesses. The conservation of volume principle under steady state conditions yields extrusion widths that are in line with the virtual nozzle slicer set point. In an experiment, we extruded multiple lines of different widths ranging from 0.4 mm to 1.0 mm, all of which were done using a 0.4 mm nozzle. Figure 27 shows the 10 mm high printed lines using a Prusa MINI (Prague, Czech Republic) and PETG filament (Polymaker Polylight PETG, Shanghai, China).

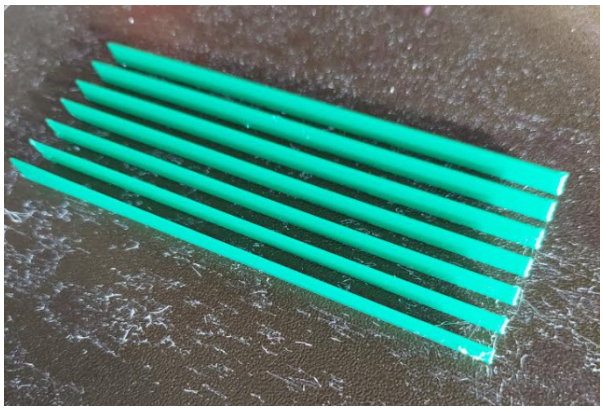

Figure 27 Printed lines using the virtual nozzle concept.

Virtual Nozzle Diameter (mm)	Actual Line Width (mm)	Relative Error %
0.4	0.400	~0 %
0.5	0.500	~0 %
0.6	0.600	~0 %
0.7	0.690	~1.4 %
0.8	0.795	~0.63 %
0.9	0.910~0.950	~3.3 %
1.0	1.00~1.04	~2 %

Table 2 Extruded line widths using virtual nozzles.

The results of this small experiment show accurate extrusion widths for the mid-section of the extruded line, away from the instabilities at the beginning and end of the lines. While Linear Advance provided better control over the start and end points, it does not provide a complete solution for our virtual nozzle system. To highlight this problem, a cube section was printed using a 0.80 mm x 0.60 mm line width and height of the infill, respectively. Meanwhile, the single outer perimeter was set as an 0.40 mm x 0.10 mm line width and height, respectively.

The Linear Advance calibration procedure was produced for a virtual nozzle of line width of 0.8 mm. The calibration G-code was a modified version of the one that is provided by Linear advance. The modifications include a higher extrusion volume equal to a theoretical rectangular extrusion of the required length. Moreover, the layer height was set as 0.3 mm. The resulting calibration run is shown in Figure 28.

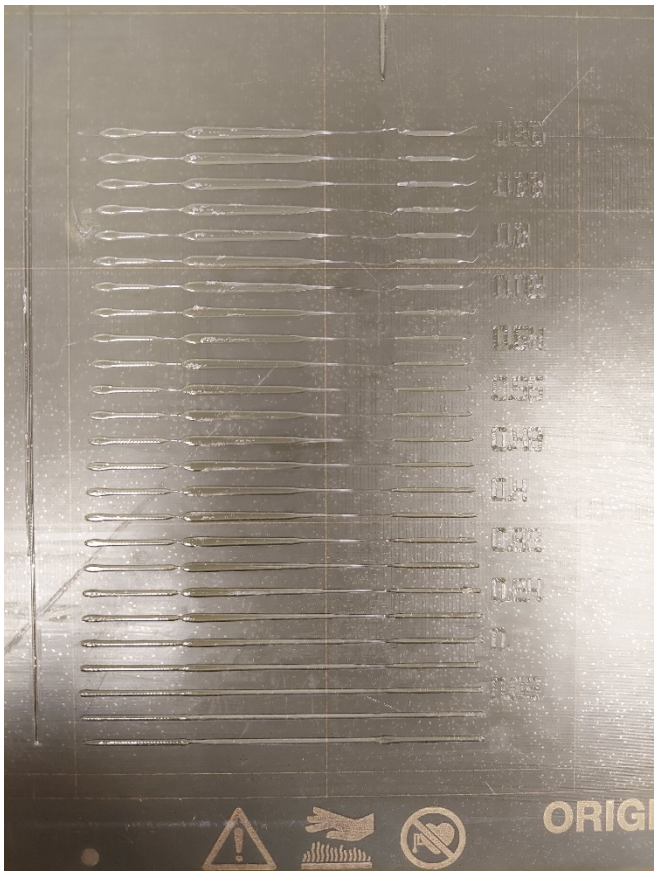

Figure 28 K value calibration print.

The resulting K value was plugged into the G-code for the infill section only. The results show that even for a well calibrated K value for all the virtual nozzle diameters, the resulting print shows clear over extrusion artifacts at the instances where the printer switches from the 0.80 mm line width process to the 0.40 mm process. This over extrusion is due to residual

pressure from the 0.80 mm process that is carried over to the 0.40 mm process. Figure 29 shows the repeating over extrusion artifacts on the 0.40 mm outer perimeter of the print.

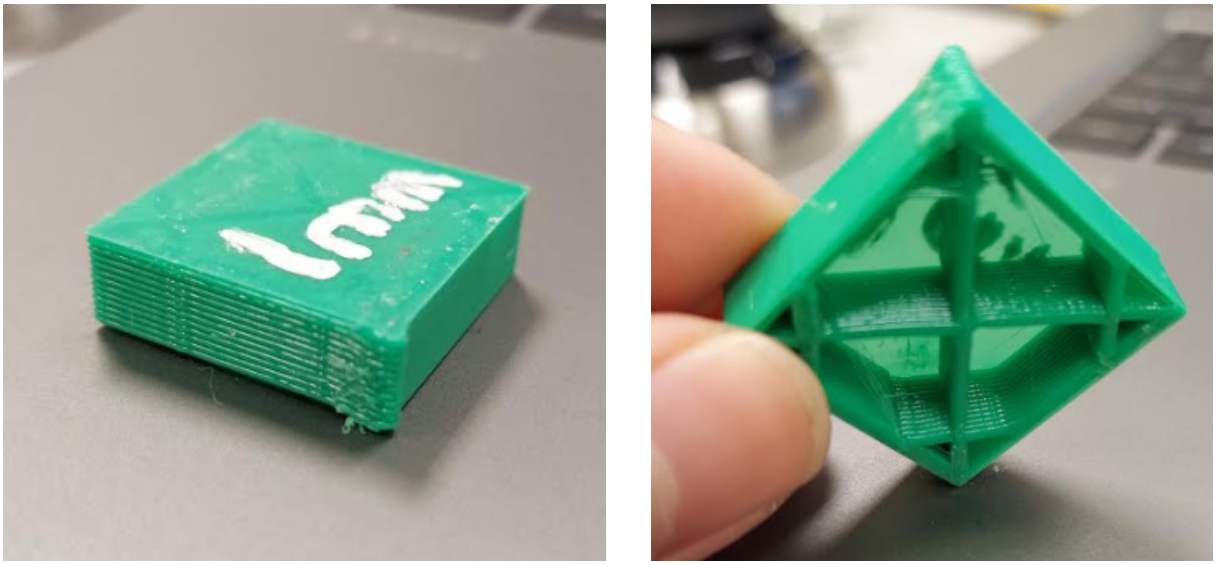

Figure 29 Over extrusion artifacts due to residual pressure and a poorly performing model.

While the infill printed with the correct layer width and height, the artifacts on the outer wall show the need for a more accurate model of the extrusion dynamics.

5.3 Time Savings Using the Virtual Nozzle System

A simple experiment was run to test the efficacy of the Virtual Nozzle system and was conducted using the same cubic object. The test objects are shown in Figure 30.

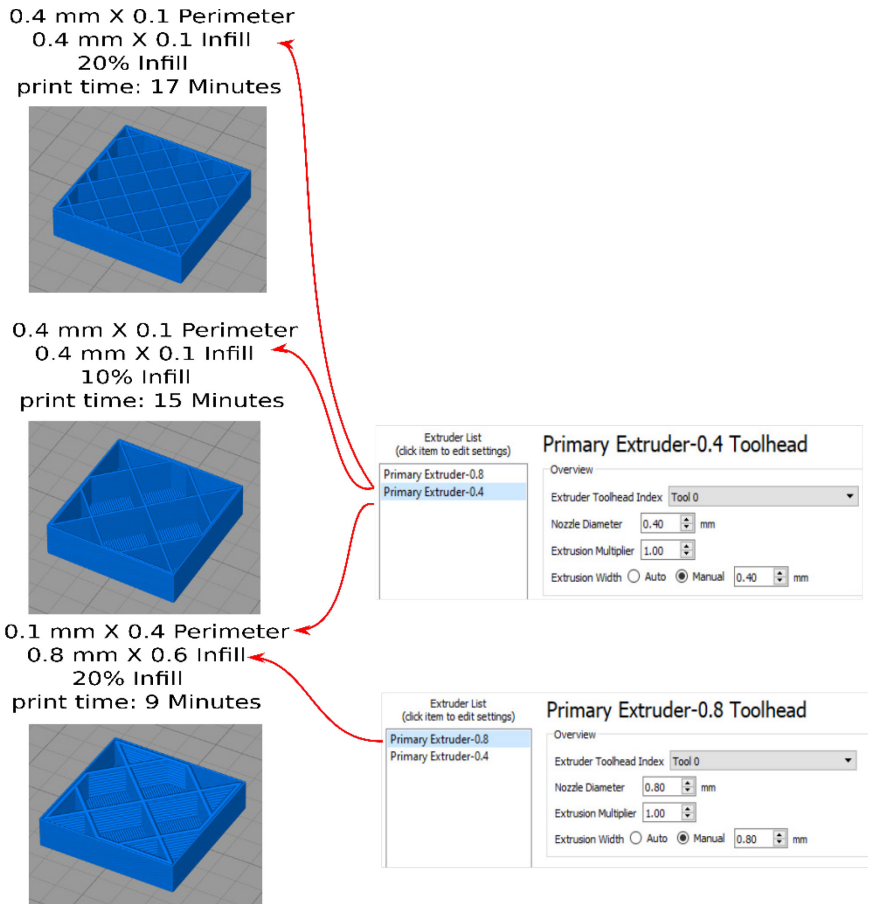

Figure 30 Print time for a half cube object using standard and virtual nozzle settings.

The first two test coupons are printed using a 0.4 mm nozzle for the infill and outer perimeter. The infill for the third test coupon is printed using a 0.8 mm virtual nozzle. From the simulated print time, for the same infill percentage, the object printed using the virtual nozzle requires 47% less print time. If the printed object is to have the same number of tool paths, the time reduction is 40%. This demonstrates the huge potential of an optimized slicing and extrusion algorithm for reducing build time while maintaining quality. Most importantly, such benefits are gained without the need for any hardware modifications. This virtual nozzle system could have another unexpected positive effect on the strength of the printed part. From literature, the UTS of an ABS dog-bone tensile test sample was increased by 9% following the change of

the nozzle diameter from 0.4 mm to 0.8 mm (Vicente & Leite, 2020). With the virtual nozzle system, this strength increase could be gained without changing the installed nozzle.

5.4 Setup of the Virtual Nozzle Extrusion System

Current common slicing software packages do not provide a great flexibility in selectively varying the extrusion width and height within the same print. Some software packages provide a variable layer height for the same object, where sections of the print can be setup to have a different layer height than the rest of the print. This feature however is limited in its scope. If we were to apply the concept of a virtual nozzle, we require a software package that can vary the extrusion width and height simultaneously for specific features of the print. For example, the half cube test required that the infill have different print settings from the outer perimeters. This level of customization was only possible with the slicing software Simplify3D. Our work takes advantage of "loopholes" that exist in the software. As shown in Figure 25 multiple extruders with varying virtual diameters can be configured within a single process, the infill, supports, skirt, and brim can be assigned to any of the previously assigned extruders. However, this work-around does not allow for the selection of a nozzle of a different size for the inner perimeters. Inner perimeters number is an important feature to have as it allows the user to maintain high resolution on the outside of the print while maintaining strength of the part by having thick and wide inner perimeters. Moreover, this method does not allow for the "continuous" variation of the output virtual nozzle diameter. Therefore, it has a similar limitation to the VOE V1.0 and V2.0.

5.5 Excess Pressure Release Using Ooze Shields

Ooze shields are a built-in feature available in most slicing software packages. The feature creates a wall like perimeter outside the object being printed. The user can dictate how wide the wall be and how far it is offset from the object. This feature is traditionally used with multi extruder systems, where the wall provides a barrier from stay oozed strands of filament from the idle extruder. In our use case, the ooze shield is used as a tool to relief the residual pressure in the extruder prior to the transition to the thinner extrusion section (outer perimeter). For the same half cube, the ooze shield provided reduced over extrusion artifacts and improved the surface finish considerably.

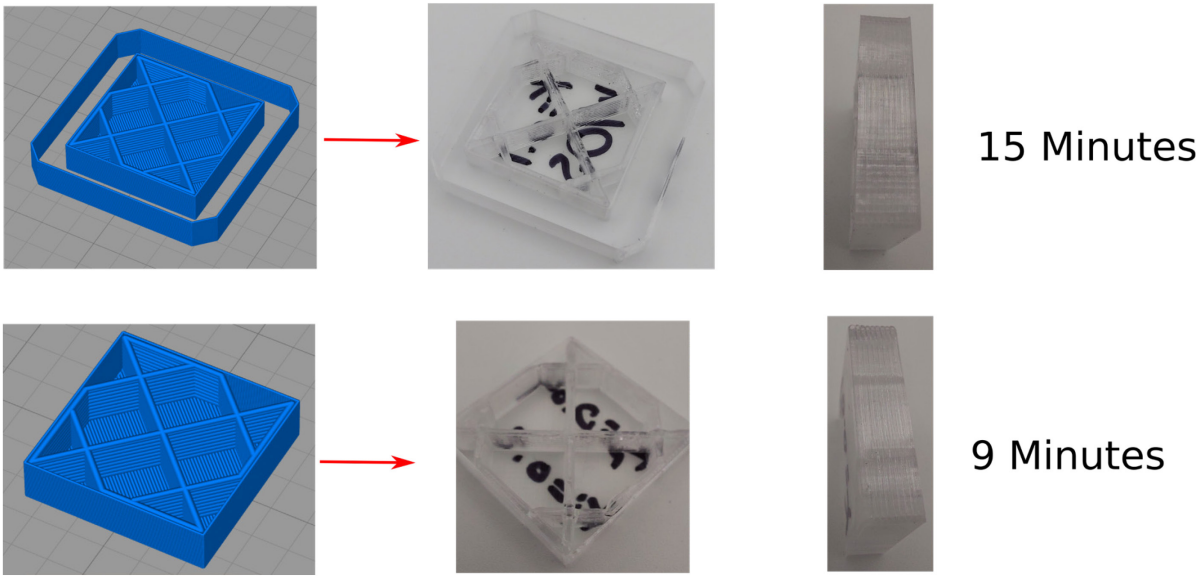

Figure 31 Half cube print results using an ooze shield.

Figure 31 demonstrates the short coming of this method, a 40% increase in print time when compared to a print without an ooze shield. This shows that this method can be a viable solution, however, it is at a cost of additional material and additional print time.

5.6 Extruder Modeling

Prior to mathematical modeling of the system, we attempted to study the behavior of the extrusion system under various extrusion speeds. The slicer generated G-code specifies the extruder speed depending on the required volumetric flow rate. The print consisted of straight lines printed with the speeds that are noted in Figure 27. The extruder pushes material at a steady volumetric flow rate for 100 mm, at which point the extruder is shut off and the excess pressure is steadily relieved over a 40 mm distance.

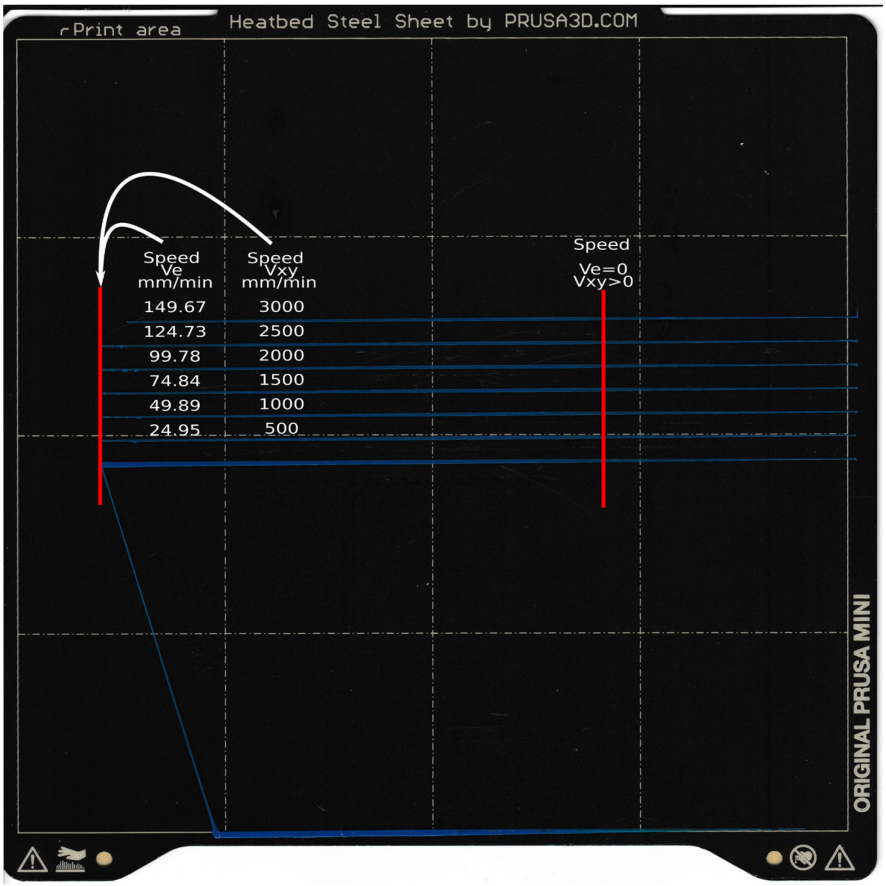

Figure 32 Extrusion pressure decay test.

The resulting test plate is scanned using a standard photocopier at a resolution of 600 dpi. The scan is then imported into ImageJ where a Local Thickness analysis is run to obtain the extruded line thickness Vs. Time. The profile of each line is then plotted using the Plot Profile

tool in ImageJ and exported as a .csv file. This file is then imported into MATLAB and a first order exponential model is curve fitted to each line profile. The time constant is then extracted from the fitted line. The resulting time constants show a decreasing value with the increase of the volumetric flow rate. This variation of the time constant depending on the feed rate shows the non-linear behavior of the extruder system.

```
Time_Constant_05 = 4.9855
Time_Constant_06 = 3.3186
Time_Constant_07 = 1.3004
Time_Constant_08 = 0.9080
Time_Constant_09 = 0.8433
Time_Constant_10 = 0.6092
```

Figure 33 Resulting time constants.

Chapter 6 Conclusion

VOE and CVOE systems have the potential in reducing print time while maintaining resolution. They can provide discrete output diameter variation via a turret, concentric cylinders, multi printheads and other methods. VOE systems can also be used for redundancy, multiple nozzles of the same size can be installed on a system like the turret-based system that we demonstrated. If the printer detects a clog via an encoder wheel, the printer can automatically switch to a functioning nozzle. While the system we demonstrate is bulky in nature, alternative and more novel designs such as our Solenoid-free design can help reduce its mass and ensure higher reliability. Yet, all VOE systems have an unsolvable limitation; extrusion must be interrupted for the switching operation to commence. This manifests itself physically as a void artifact in the print, moreover, it consumes build time for each nozzle switching operation. CVOE systems build upon what VOE system provide without the need for switching operations. They provide a continuous range output cross sectional area even while extruding. This feature however comes at the cost of mechanistic complexity and the need for high tolerance parts and mechanisms. We introduce the concept of a novel VCVOE system that requires little to no hardware modification yet provides some of the benefits and times savings that a mechanical CVOE system can provide. Relying on novel slicing algorithms and high-fidelity models of extruder dynamics, CVOE type behavior can achieved using standard hobbyist level printer hardware. Using this system however requires a good understanding of the limitations of each printer model as physical flow rate limitations put a limit on its usefulness. It is important to note

that both the VOE and CVOE systems are only as useful as the slicer software that will make use of their capability. Slicing algorithms and extruder dynamics modeling are the next topic of research for this project.

Future Work

As with any highly experimental work, results can steer the work in new and unexpected directions. This was no different in our work on Variable Orifice and Variable extrusion systems. From our work so far, it has become abundantly clear that more accurate modeling of the extruder dynamics will be an important step to complete not only for the “virtual nozzle” concept, but for the mechanical CVOE system as well.

With that work, slicer development should commence to make use of the newfound capabilities that the CVOE system can provide. Novel slicing behaviors can be programed in like interlocking layers, where a single extrusion increases in width and height which, in theory, should provide some novel mechanical properties.

Following the completion of the modeling and build of the system, attention should be given to the mechanical properties of the parts produced by the CVOE system. This includes, tensile, impact, flexure, hardness, shear, fatigue testing of samples printed on the CVOE system using NIST standard protocols.

References

Brooks, H., Rennie, A., Abram, T., McGovern, J., & Caron, F. (2011). Variable fused deposition modelling - concept design and tool path generation. *12th Rapid Design, Prototyping & Manufacturing Conference*, 113–122. https://doi.org/10.13140/2.1.2280.2887

Chesser, P., Post, B., Roschli, A., Carnal, C., Lind, R., Borish, M., & Love, L. (2019). Extrusion control for high quality printing on Big Area Additive Manufacturing (BAAM) systems. *Additive Manufacturing*, *28*, 445-455. https://doi.org/10.1016/j.addma.2019.05.020

Espalin, D., Ramirez, J., Medina, F., & Wicker, R. (2014). Multi-material, multi-technology FDM system: exploring build process variations. *Rapid Prototyping Journal*, *20*(3), 236-244. https://doi.org/10.1108/RPJ-12-2012-0112

Fayazbakhsh, K., Movahedi, M., & Kalman, J. (2019). The impact of defects on tensile properties of 3D printed parts manufactured by fused filament fabrication. *Materials Today Communications*,*18*, 140–148. https://doi.org/10.1016/j.mtcomm.2018.12.003

Kostic, M. M., & Reifschneider, L. G. (2006). Design of Extrusion Dies. *Encyclopedia of chemical processing,* Taylor & Francis. https://doi.org/10.1201/NOE0824755638

Lind. Randall F, Post. Brian K., Love. Lonnie J., Lloyd. Peter D, Carnal. Charles Lynn, Blue. Craig A., Kunc. V. (2016). *Variable Width Deposition for Additive Manufacturing with Orientable Nozzle*. US 20170320267A1, United States Trademark and Patent Office.https://patents.google.com/patent/US20170320267A1/en

Myerberg, J., Fulop, R., Gibson, M., Hart, A., Fontana, R., & Schuh, C. et al. (2018). *Fused Filament Fabrication Nozzle With Controllable Exist Shape*. US 20180311738A1, United States Trademark and Patent Office. https://patents.google.com/patent/US20180311738A1/en

Rajamani, P. K., Ageyeva, T., & Kovács, J. G. (2021). Personalized mass production by hybridization of additive manufacturing and injection molding. *Polymers*, *13*(2), 1–19. https://doi.org/10.3390/polym13020309

Thomas, D. & Gilbert, S. (2014). Additive manufacturing costs and benefits. In *Costs and cost effectiveness of additive manufacturing* (pp. 11-46). National Institute of Standards and Technology. Retrieved from https://nvlpubs.nist.gov/nistpubs/SpecialPublications/NIST.SP.1176.pdf

Tronvoll, S. A., Popp, S., Elverum, C. W., & Welo, T. (2019). Investigating pressure advance algorithms for filament-based melt extrusion additive manufacturing: theory, practice and simulations. *Rapid Prototyping Journal*, *25*(5), 830–839. https://doi.org/10.1108/RPJ-10-2018-0275

Tseng, A. A., & Tanaka, M. (2001). Advanced deposition techniques for freeform fabrication of metal and ceramic parts. *Rapid Prototyping Journal*, *7*(1), 6–17. https://doi.org/10.1108/13552540110365117

Vicente, C. M. S., & Leite, M. (2020). Influence of fused deposition modeling parameters on the mechanical properties of ABS parts. *Polymers for Advanced Technologies*, *31*(3), 501–507. https://doi.org/10.1002/pat.4787

Wang, T., Chang, L., FANG, Y., & Lin, Y. (2018). *Feeding device and variable squeezing mouth for 3d printing*. US 20180154586A1, United States Trademark and Patent Office. https://patents.google.com/patent/US20180154586A1/en

Xu, J., Ding, L., Cai, L., Zhang, L., Luo, H., & Qin, W. (2019). Volume-forming 3D concrete printing using a variable-size square nozzle. *Automation in Construction*, *104*, 95–106. https://doi.org/10.1016/j.autcon.2019.03.008